International Journal of Pharmaceutics: X 5 (2023) 100179

Contents lists available at ScienceDirect

International Journal of Pharmaceutics: X

journal homepage: www.sciencedirect.com/journal/international-journal-of-pharmaceutics-x

3D printing of amorphous solid dispersions: A comparison of fused deposition modeling and drop-on-powder printing

Nadine Gottschalk [a,b], Malte Bogdahn [b,*,1], Julian Quodbach [a,c,1]

[a] Institute of Pharmaceutics and Biopharmaceutics, Heinrich Heine University, Düsseldorf, Germany
[b] Merck KGaA, Darmstadt, Germany
[c] Department of Pharmaceutics, Utrecht Institute for Pharmaceutical Sciences, Utrecht University, Netherlands

ARTICLE INFO

Keywords:
Fused deposition modeling
Drop-on-powder
Binder jetting
Amorphous solid dispersion
Solubility enhancement
3D printing
Additive manufacturing

ABSTRACT

Nowadays, a high number of pipeline drugs are poorly soluble and require solubility enhancement by e.g., manufacturing of amorphous solid dispersion. Pharmaceutical 3D printing has great potential in producing amorphous solid oral dosage forms. However, 3D printing techniques differ greatly in terms of processing as well as tablet properties. In this study, an amorphous formulation, which had been printed via Fused Deposition Modeling and drop-on-powder printing, also known as binder jetting, was characterized in terms of solid-state properties and physical stability. Solid state assessment was performed by differential scanning calorimetry, powder X-ray diffraction and polarized microscopy. The supersaturation performance of the amorphous solid dispersion was assessed via non-sink dissolution. We further evaluated both 3D printing techniques regarding their processability as well as tablet uniformity in terms of dimension, mass and content. Challenges and limitations of each 3D printing technique were discussed. Both techniques are feasible for the production of amorphous formulations. Results indicated that Fused Deposition Modeling is better suited for production, as the recrystallization tendency was lower. Still, filament production and printing presented a major challenge. Drop-on-powder printing can be a viable alternative for the production of amorphous tablets, when a formulation is not printable by Fused Deposition Modeling.

1. Introduction

The majority of new drug entities nowadays is poorly soluble. It is estimated that poorly soluble compounds make up around 70% of pipeline compounds (Ting et al., 2018). One of the most used techniques to enhance their solubility is the production of amorphous solid dispersions (ASD). The amorphous state is unstable and can be stabilized by polymers. The incorporation of an active pharmaceutical ingredient (API) can be performed e.g., by hot-melt extrusion (HME) in which the API and polymer are transformed into the amorphous state by means of thermal and mechanical energy (Shah et al., 2014). Regarding the production of solid oral dosage forms (SODF) a classical process chain would be to mill the extrudate, add additional excipients and perform tableting. In early clinical trials, this can lead to issues as different dosages are in evaluation, requiring different tablet formulations. Formulation development can be challenging especially in early stages of development because only small quantities of active pharmaceutical ingredient (API) are available.

Novel manufacturing techniques, such as three-dimensional printing (3DP), can be valuable for the pharmaceutical industry, due to fast adaptability of the 3D tablet design. Among the wide range of 3DP techniques, the most reported techniques to produce SODFs are Fused Deposition Modeling (FDM), due the good availability of affordable printers (Araújo et al., 2019), and drop-on-powder (DoP) printing, being the first 3DP technique to result in a FDA approved pharmaceutical product (Vaz and Kumar, 2021).

Abbreviations: 3DP, three-dimensional printing; ACN, acetonitrile; API, active pharmaceutical ingredient; ASD, amorphous solid dispersion; CAD, computer-aided design; CV, coefficient of variation; DoP, drop-on-powder; dpmm, dots per millimeter; DSC, differential scanning calorimetry; FaSSIF, fasted state simulated intestinal Fluid; FDM, fused deposition modeling; T_g, glass transition temperature; HME, hot-melt extrusion; KTZ, ketoconazole; pXRD, powder X-ray diffraction; SODF, solid oral dosage form; UPLC, ultra-performance liquid chromatography.

* Corresponding author.
E-mail address: Malte.Bogdahn@Merckgroup.com (M. Bogdahn).
[1] Both authors contributed equally.

https://doi.org/10.1016/j.ijpx.2023.100179
Received 28 December 2022; Received in revised form 16 March 2023; Accepted 17 March 2023
Available online 20 March 2023

FDM belongs to the material extrusion processes. Filament, the wirelike feedstock material, is pushed through a heated nozzle and the 3D object is created through layer-by-layer deposition of molten material. In FDM, the mechanical properties of filaments are of great importance as they are decisive for printability (Fuenmayor et al., 2018; Ilyés et al., 2019; Nasereddin et al., 2018; Zhang et al., 2017). The mechanical properties depend on different factors, such as the type and proportions of API, polymer and additional excipients. FDM, as a melt-based manufacturing method, is well suited for the production of ASDs. Amorphization of the API can be achieved either during HME or during the printing process (Prasad et al., 2019). Several studies have demonstrated the possibility to produce amorphous FDM-printed SODFs (Buyukgoz et al., 2021; Gottschalk et al., 2021; Jamróz et al., 2018; Kissi et al., 2021; Prasad et al., 2019).

DoP printing can be referred to the additive manufacturing category binder jetting and is part of the powder-based 3DP techniques. Ink droplets are generated and jetted onto powder layers. The ink fuses powder particles in-situ, resulting in porous systems. Polymeric binders are necessary to provide the required mechanical stability of the tablet and can be included in the ink (Chang et al., 2021; Yu et al., 2009) as well as in the powder bed (Antic et al., 2021; Infanger et al., 2019). There is also the possibility to include the API in the ink (Clark et al., 2020; Wickström et al., 2015). Solvent evaporation from droplets can be fast and similar to other solvent evaporation methods like spray drying, ASDs can be produced. However, this kind of binder jetting is mainly restricted to printing on edible paper or of oral films instead of powder-based dosage forms. Due to this, the achievable dosages in the final SODFs are low (Clark et al., 2020; Raijada et al., 2013; Wickström et al., 2015). In contrast, adding the API to the powder bed enables high drug loads up to 70% but is mainly limited to highly soluble drugs (Infanger et al., 2019; Wang et al., 2021). Recently, we published a printing approach, which uses milled extrudate as powder bed material to enable higher drug loadings up to 40% of a poorly soluble API in its amorphous form (Gottschalk et al., 2022a) and on which we will elaborate further in this study.

Both techniques, FDM and DoP printing, can be used to produce amorphous SODFs. In this study we directly compare these techniques by using exactly the same raw material, a hot-melt extruded ASD. We demonstrate opportunities and challenges that arise during material processing and the influence of the different printing techniques on tablet properties and physical stability of an ASD. The poorly soluble API ketoconazole (KTZ) was used as model compound. Copovidone was used due to its versatile use as a matrix former for ASDs as well as good binding capacities in DoP printing. Process development was described in an earlier study on DoP printing (Gottschalk et al., 2022a) and FDM (Gottschalk et al., 2022b; Gottschalk et al., 2021) and optimized printing conditions were applied. This study is meant to display the advantages and disadvantages of each technique and act as a decision guide for drug product development.

2. Material and methods

2.1. Materials

KTZ was used as model compound. KTZ is poorly soluble (0.08 mg/mL in phosphate buffer pH 6.8 (Ullrich and Schiffter, 2018)) and melts at 151 °C (Kanaujia et al., 2011). KTZ was purchased from LGM Pharma (Boca Raton, USA). Copovidone, which was used as matrix polymer (Kollidon® VA64, vinylpyrrolidone-vinyl acetate copolymer), was purchased from BASF (Ludwigshafen, Germany). Colloidal silicon dioxide was used as flowability enhancer and was purchased from Evonik Industries (Essen, Germany).

Fasted State Simulated Intestinal Fluid (FaSSIF) powder was purchased from Biorelevant.com Ltd. (London, UK). Hydrochloric acid (HCl, 0.1 M), acetonitrile (ACN, hypergrade, purity ≥99.9%), sodium hydroxide solution (1 M), formic acid, ammonia solution (25%), sodium chloride and di-sodium hydrogen phosphate were purchased from Merck KGaA (Darmstadt, Germany). All reagents used in this study were of analytical grade.

2.2. Extrusion and filament production

The powder blend was prepared using a Turbular® mixer (T2C, Willy A. Bachofen AG, Muttenz, Switzerland). First, KTZ (20%) and copovidone (79%) were blended for 15 min. Hereafter, colloidal silicon dioxide (1%) was added to the premix and blended for another 15 min.

Extrusion was performed on a Pharma 11 hot-melt extruder (Thermo Fisher Scientific, Waltham, USA) with a 1.75 mm die with a length of 3 cm. The screw configuration consisted of three mixing elements to achieve good mixing of all components. The detailed screw configuration is displayed in the supplementary material (Table S1). Heating zone 1 was set to 60 °C, zone 2 to 120 °C, zones 3–7 to 180 °C and the die to 175 °C. Feeding was performed using a gravimetric feeder (Congrav® OP 1 T, Brabender Technologie GmbH & Co. KG, Duisburg, Germany) at 0.2 kg/h. The screw speed was set to 300 rpm. A conveyor belt (Brabender Technologie GmbH & Co. KG, Duisburg, Germany) was used to adjust the filament diameter to 1.75 mm by adapting the conveyor belt speed. The diameter was measured using a laser axis measurement system (Odac Trio33, Zumbach Electronic AG, Orpund, Switzerland). The intended filament diameter was 1.75 mm ± 0.05 mm and only filament within this specification was used for FDM printing.

2.3. Feed force testing

The feed force tester as described in Gottschalk et al. (2022b) was used to determine suitable printing conditions on a Texture Analyser (TA-XT, Stable Micro Systems, Godalming, UK). A test speed (piston movement speed) of 1.00 mm/s was chosen, which equals a printing speed of 30 mm/s. For further details see Gottschalk et al. (2022b). Tests were performed in quintuplicate at 130 °C, 140 °C and 150 °C. Feed forces were determined in the last 40 mm of testing distance.

2.4. Printing FDM

Printing was performed on an Ultimaker 3 (Ultimaker, Utrecht, Netherlands) equipped with an Ultimaker print core (0.4 mm, BB). The printer had been modified according to Gottschalk et al. (2021) to enable the printing of brittle filaments as well as printing with a filament diameter of 1.75 mm. The tablet design was cylindrical and was created in Fusion 360 (Autodesk, San Rafael, USA) with a height of 2.4 mm and a diameter of 10 mm. The design was saved as binary stereolithography file format (.stl). Slicing was performed using Simplify3D (version 4.0.1., Simplify3D, Cincinnati, USA). The nozzle was heated to 150 °C and the build plate up to 70 °C. Printing was performed at 30 mm/s, a line width of 0.4 mm and a layer height of 0.2 mm. The infill density was 100%. Printed tablets are referred to as FDM tablets in the following text.

2.5. Milling

Part of the filaments was milled to achieve fine powder for DoP printing. Samples were milled using an ultra-centrifugal mill (ZM 200, Retsch, Haan, Germany). A twelve-tooth rotor and a sieve with a mesh size of 200 µm with a distance ring were employed. Filaments were milled at 10,000 rpm. Particle size was determined using a Camsizer X2 (Retsch, Haan, Germany) equipped with the X-jet module and applying a dispersing pressure of 50 kP. Gap width was set to 4 mm. Milled powder is referred to as DoP powder in the following text.

2.6. Printing DoP

A custom-made powder bed printer was used for DoP printing of

tablets. The printer consisted of a powder reservoir, a roller for powder deposition, a building platform, which can be controlled in *xyz*-direction, and a fixed printhead, a modified HP C6602 cartridge. The printer setup is described in detail in Gottschalk et al. (2022a). The same computer-aided design (CAD) file as in 2.4. was used for printing of DoP tablets. Slicing was performed with an in-house developed script. Tablets were printed at 30 dots per mm (dpmm) in printing direction with an ink containing ethanol and water (70:30 wt%) and an infill density of 100%. The parameters had been determined in a previous study and have been selected since the settings led to best results regarding mechanical properties and solid state. Printed tablets are referred to as DoP tablets in the following text.

2.7. Tablet dimension and mass

Tablet height and diameter were determined using a digital caliper (TWIN-Cal IP67, TESA Technology, Renens, Switzerland) for all printed tablets. Measurements were performed in triplicate. Tablet mass of all tablets was determined using an analytical balance (ME235S-0 CE, Sartorius, Goettingen, Germany).

2.8. Differential scanning calorimetry (DSC)

Blend, filament, tablets and DoP powder were analyzed regarding their solid state with a DSC 1 (Mettler Toledo, Gießen, Germany). Filament (approximately 500 mg) and tablets (3 each) were ground using mortar and pestle. Approximately 7–8 mg were weighed into 100 µL aluminum pans and sealed. The lid was pierced prior to the analysis using the automatic piercing unit. A pierced pan was used as reference. Two heating cycles from 0 to 170 °C were applied at 10 K/min.

2.9. Powder X-Ray diffraction (pXRD)

PXRD measurements were performed on ground tablets, filament and DoP powder to determine the solid state using a D2 Phaser (Bruker, Billerica, USA) equipped with an SSD160 detector in 1D mode. A full opening of 4.875° was used. A copper anode at 30 kV and 10 mA was used to generate X-rays. Reduction of Kβ radiation was done by nickel foil. Sample preparation was performed on a zero-background holder with well. Sample rotation speed was set to 5 rpm and sample was scanned from 6° to 35° with a step size of 0.02° and measurement time of 6 s per step.

2.10. Polarized light microscopy

Ground tablets, filament and DoP powder were analyzed in white and polarized light under a microscope (IX73P1F, Olympus, Tokyo, Japan) at 5× and 10× magnification for the detection of crystalline traces. In addition to that, the powder raw materials were assessed regarding their particle size in white light at 10× magnification. Microscopical images were recorded and evaluated using Olympus cellSens Standard software (version: 1.18).

2.11. Content

KTZ concentration was determined using ultra-performance liquid chromatography (UPLC). The method is described in (Gottschalk et al., 2021). FDM and DoP tablets were assessed as well as the corresponding feedstock materials (filament and DoP powder). Regarding filament, coherent pieces were analyzed instead of milled samples to assess possible effects on API distribution. Samples were weighed into small glass vessels and diluted with a mixture of ACN and MilliQ water (50:50) to a concentration of 0.2 mg/mL (assuming a drug load of 20% KTZ). Tests were performed in triplicate.

2.12. Non-sink dissolution

Non-sink dissolution of tablets, filament and milled filament was performed in FaSSIF. FaSSIF was prepared by using FaSSIF powder at a concentration of 22 mg/mL in phosphate buffer pH 6.5. Ground samples were accurately weighed using a micro balance (MCA6.6S-2S00-M Cubis®, Sartorius, Goettingen, Germany) into 2 mL Eppendorf caps (approximately 3 mg). By adding 1.2 mL of heated FaSSIF (37 °C) the experiment was started. First, samples were vortexed for 30 s (Vortex-Genie® 2, Scientific Instruments, Schwäbisch Gmünd, Germany) and placed in an incubator (Thermomixer comfort, Eppendorf, Hamburg, Germany) heated up to 37 °*C*. Prior to each sampling point, samples were centrifuged at 15,000 rpm (Mikro 200R, Hettich, Tuttlingen, Germany). At each sampling point 50 µL of supernatant was removed and diluted with 50 µL of ACN to prevent precipitation. The cycle of vortexing, incubation and centrifugation was repeated after each sampling. The removed volume was not replaced. Sampling points were 5, 10, 15, 20, 30, 45, 60, 90 and 120 min. The maximum possible API concentration was 500 µg/mL. Tests were performed in triplicate.

2.13. Sink-dissolution

Dissolution was performed according to the Ph. Eur. 2.9.3. and 5.17.1. in a dissolution tester (Smart AT7, Sotax, Aesch, Switzerland) equipped with paddles (USP dissolution apparatus 2). Paddle rotation speed was set to 100 rpm. DoP and FDM tablets ($n = 3$, respectively) were dissolved in 900 mL of 0.1 N HCl at 37 °C. 3 mL of sample was drawn at 5, 10, 15, 30, 45, 60, 90 and 120 min. Sink-dissolution was performed with the aim to investigate differences in terms of drug release from the different dosage forms. As the surface area to volume ratio strongly influences the release (Windolf et al., 2021), the same tablet designs were compared. However, as printing resulted in different tablet weights, the absolute API mass differed, being approximately 48 mg for FDM printed tablets and approximately 30 mg for DoP printed tablets.

2.14. Three-point bending test

The three-point bending flexural test is commonly applied to assess and compare the mechanical properties of filaments for the FDM process. A Texture Analyser TA-XT equipped with a three-point bending rig (Stable Micro Systems, Godalming, UK) was used. The gap between the supports was 30 mm. The test punch was moved at 5 mm/s prior to the test and reduced to 0.1 mm/s upon contact with the test specimen. Filament diameter was assessed using the laser measurement system (Section 2.2) prior to the test and stress and strains were calculated for each run. Tests were carried out in tenfold. The strain at break was determined to evaluate the brittleness of the material. Data were acquired using Exponent software (version 6.1.16.0).

2.15. Material density

Extrudate density was analyzed using a nitrogen pycnometer (Ultrapyc 1200e gas expansion pycnometer, Quantachrome, Boynton Beach, USA). The target pressure was 1.4 bar. Extrudate was milled using a Tube Mill Control (IKA, Staufen, Germany) at 25,000 rpm. Tests were performed in triplicate and approximately 4–5 g of sample were analyzed in each run.

2.16. Storage conditions

Samples of each feedstock material (filament and DoP powder) and tablets (FDM and DoP) were placed in glass vessels and stored for 2, 4 and 12 weeks in a desiccator in a climate chamber (KBF 240, Binder, Tuttlingen, Germany) at 40 °C.

3. Results and discussion

3.1. Processing

In FDM, filament diameter homogeneity is of great importance as fluctuations >1.75 m ± 0.05 mm may lead to deviations in tablet mass (Ponsar et al., 2020). The filament diameter during extrusion is displayed in Fig. 1. It shows that the diameter was not always in the range of 1.75 mm ± 0.05 mm. The filament diameter was manually adapted by adjusting the speed of a conveyor belt. A small die swell was observed at the extruder die, wherefore stretching of the extrudate strand was necessary. To find the appropriate conveyor belt speed was difficult and a trial-and-error process. Oscillating fluctuations in diameter were observed approximately every 30–60 s. These signals did not correlate with other extrusion parameters such as torque, die pressure or actual throughput as these were constant (supplementary material Fig. S1). Earlier extrusion experiments on the Pharma 11 had also shown these oscillations and it is assumed that these are likely a result of the pulsatile material transport in twin-screw extruders, which is correlated to high screw speeds (Ponsar et al., 2020). High screw speeds of 300 rpm were used in this setup as they have been reported to be a critical parameter for the production of ASDs. They provide mechanical energy input and facilitate molecular dispersion of the API in the polymer matrix (Keen et al., 2014) as well does the use of kneading zones. It was shown that the use of three kneading zones in the screw configuration, which was the case in this study, leads to discontinuous material transport and fluctuations in filament diameter (Chamberlain et al., 2022). For the following experiments it was important to use fully amorphous material. In case of FDM printing it was assumed that the short residence in the hot end would not provide sufficient thermal energy to amorphize the API. Since the extruded material was also used as starting material for DoP printing, it was necessary that the API was fully amorphous and well distributed in the polymer matrix since crystalline traces and local supersaturation were likely to result in recrystallization upon contact with the ink. Due to that, higher diameter fluctuations were accepted during extrusion. However, FDM printing of tablets was performed only with selected filament within the specification of 1.75 mm ± 0.05 mm to reduce tablet mass deviations.

The FDM printing temperature was determined using the feed force tester. Forces below the printer force limit of 4 N were achieved at 140 °C. Even though the melt flow was suitable at 140 °C, printing had to be performed at 150 °C as the material did not stick to the build plate. Tablets detached during printing, stopping the printing process.

Handling indicated that filament was very brittle. The strain at break determined via the 3-point bending test was low (2.5% ± 0.6%) and further decreased during storage at accelerated conditions to 1.5–1.7% (Table 1). The decrease in breaking strength was a result of fine hairline cracks (supplementary material Fig. S2), which had formed during storage in a desiccator at 40 °C, most likely a result of subsequent drying (see chapter 3.3.). In FDM, suitable mechanical properties of the filament are crucial for their printability.

The brittleness of the material was beneficial for the production of DoP powder bed material as it facilitated milling to a small particle size without the use of liquid nitrogen. However, milling was only possible batchwise as the fine particles did block the sieve after approximately 1 h. The milling chamber reached up to 50 °C during milling. Milled powder proved easy to in handling during printing. As described in Gottschalk et al. (2022a), milled extrudate was easily spreadable over a broad range of settings and resulted in a smooth powder bed. The only drawback here was the hygroscopicity of the material combined with a high surface area of the finely milled material. Water sorption led to attachment of particles to the roller-recoater system, which had to be removed manually before each layering process.

3.2. Tablet properties

Due to the different manufacturing processes, tablet appearance differed strongly between FDM and DoP printed tablets. FDM tablets had a glassy appearance and were transparent (Fig. 2). Grooves from the printer nozzle were clearly visible on the tablet surface and tablet edges were sharp. In contrast, DoP tablets were white and had a powdery surface. Edges were slightly rounded compared to FDM tablets. Darker lines on the tablet surface of DoP tablets were a result of the slicer setting. The intension was to produce a slight overlap of the jetted ink to prevent tablets from falling apart at potential printing gaps. This is discussed in detail in Gottschalk et al. (2022a). In addition, the shape of these tablets was slightly elliptical compared to FDM printed tablets. The reason for this is that FDM tablets were produced by printing two circular shell layers and a rectilinear infill pattern, while DoP tablets were produced by depositing the ink as stripes, since the twelve nozzles were

Table 1
Strain at break in 3-point bending test of filaments over storage (Mean strain at break and SD, $n = 10$).

	T0	2 weeks	4 weeks	12 weeks
Strain at break (%)	2.5	1.5	1.7	1.7
SD (%)	0.6	0.5	0.2	0.2

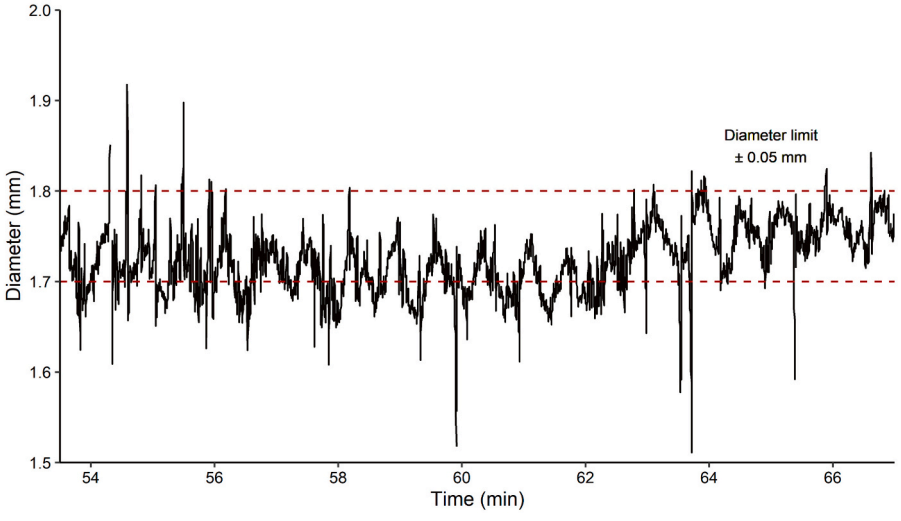

Fig. 1. Filament diameter during extrusion.

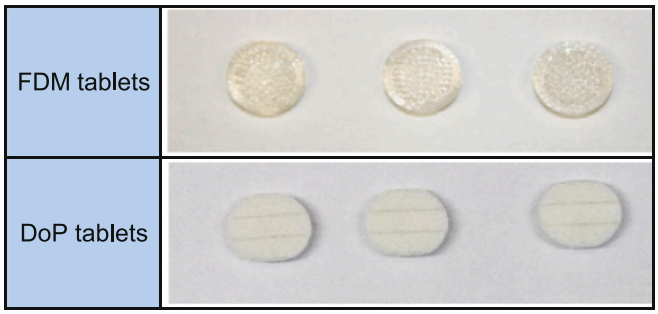

Fig. 2. FDM and DoP tablets.

arranged in line.

Printing using the same CAD file resulted in different tablet masses (Table 2). Mean FDM tablet mass was approximately 1.6× higher than DoP tablet mass. In FDM, the molten material solidifies, resulting in very dense objects with only few voids (Gottschalk et al., 2022b). The tablet mass-to-volume ratio (1.21 g/mL) corresponds approximately the material density (1.23 g/mL) of the intended 3D design. Fine powder material, which was used for DoP printing, had a smaller bulk density and, corresponding to that, tablets had a lower density (0.8 g/mL compared to 1.2 g/mL assuming mean values for tablet dimension and mass from Table 2).

The tablet height and diameter of FDM tablets were slightly elevated compared to the CAD design (approximately +0.1 mm in terms of tablet height and + 0.4 mm in terms of diameter). Elevated height is possibly a result of the bumpy tablet surface, whereas the elevated tablet diameter is possibly a result of the nozzle pushing the softened material to the sides. DoP tablet height differed between the batches and was also slightly higher compared to the CAD file design in most cases. Elevated height of DoP tablets is possibly a result of the polymer swelling upon contact with the ink. Copovidone is known to swell upon contact with water (Antic et al., 2021). The tablet diameter was only slightly lower (approximately 0.15 mm) than the target design.

Regarding the deviations in tablet mass and dimensions, differences were observed between the various batches of DoP tablets (Table 2). A maximum of twelve tablets was printed in one run. The number of suitable tablets of each run differed because some of the tablets stuck to the build plate and broke during removal. Tablets had to be printed in a way that the ink in the first layer was in contact to the build plate to reduce warping (Gottschalk et al., 2022a). Further, printing had to be performed on different days to reach the number of tablets necessary for the stability testing, whereas FDM tablets were printed within one day. Here, a number of ten tablets was defined as one batch to facilitate comparison between FDM and DoP tablets and evaluate whether there were trends during printing.

Regarding DoP tablets, a mass increase was observed between the different prints. The total difference between the first and the last batch was approximately 20 mg. However, the variations within one DoP tablet batch were significantly lower than the variations of the FDM tablets ($p < 0.05$). As described in Section 3.1., copovidone is very hygroscopic and the powder surface area was large. The powder cartridge had been stored over-night in a plastic bags, therefore it is likely that the increase in mass is a result of water sorption. The coefficient of variation (CV) of the FDM batches was higher in most cases, ranging from 1.0% - 4.4%, which can probably be attributed to filament diameter deviations. Filament was produced in a range of 1.7–1.8 mm, which can result in mass deviations up to 5.8% in theory. Mass conformity is crucial in the production of high dose SODFs as tablet mass deviations can result in dosage fluctuations. An optimized extrusion process and filament uniformity may improve the mass uniformity of printed tablets. Other factors contributing to impaired mass conformity related to the printing process may be inconsistent filament forward propulsion as a result of high viscosities in the nozzle, which can be excluded since optimized conditions according to the feed force tester were used. However, it might be possible that oozing occurred, since a higher printing temperature was necessary to ensure that tablets adhered do the build plate. Adding to that, the build plate height may be another factor. It has been shown that printed mass differed significantly when the build plate was leveled by different operators (Melocchi et al., 2016) and on different days of leveling (Alhijjaj et al., 2019). In this study leveling was performed by one person at the start of printing and was not altered until all FDM tablets required were printed. However, it is possible that build plate height changes slightly during removal of printed tablets.

3.3. Solid state and physical stability

Every step in the process chain can influence the solid state and physical stability of an ASD. Therefore, all steps from filament, milled DoP powder and printed tablets were considered. Polarized microscopic images as well as DSC measurements indicated that the feedstock materials were fully amorphous, demonstrating that extrusion was successful in producing amorphous material and furthermore, that milling did not promote recrystallization. Reheating of amorphous filaments during FDM printing did not affect the solid state either. However, small birefringence was occasionally observed for DoP printed tablets (Fig. 3). This effect was already described in our previous study and is due to local overwetting of ink. The analytical methods DSC and pXRD were not capable of detecting these small amounts of crystals, concluding that the amount was below the limit of detection of 2% and 5%, respectively, which was determined in a previous study (Gottschalk et al., 2021). During storage over twelve weeks, samples remained amorphous or, in case of DoP tablets, no further increase of recrystallization was observed (Fig. 3), which can be attributed to the porous structure of the tablets. The porous structure prevents the spread of recrystallization by forming crystallization barriers in form of voids.

Table 2
Dimensions and weight of DoP and FDM tablets for the respective batches. Number of tablets denotes the usable tablets from a batch and the total number printed in a batch. Batch numbering: first number refers to the day of printing and second number to the printing order on that day.

Tablet type	Batch	Number of tablets	Mean height (mm)	CV (%)	Mean diameter (mm)	CV (%)	Mean mass (mg)	CV (%)
DoP	1.1	3/3	2.43	2.65	9.82	1.60	138.7	0.1
	2.1	7/12	2.44	2.12	9.86	0.75	143.8	0.9
	2.2	8/12	2.41	1.75	9.80	0.45	145.3	1.2
	3.1	11/12	2.40	1.49	9.84	0.36	148.1	1.5
	3.2	12/12	2.46	2.17	9.86	0.68	149.7	1.0
	3.3	12/12	2.46	1.60	9.83	0.53	149.6	1.0
	4.1	10/12	2.50	1.22	9.85	0.49	156.3	1.1
	4.2	12/12	2.49	1.30	9.86	0.44	160.8	1.2
FDM	1.1	10	2.48	1.82	10.36	0.63	239.9	1.8
	1.2	10	2.48	1.49	10.43	0.74	240.6	1.0
	1.3	10	2.50	2.43	10.49	0.53	242.0	2.8
	1.4	10	2.53	3.32	10.44	0.71	238.4	4.4
Target value	–	–	2.40	–	10.00	–	–	–

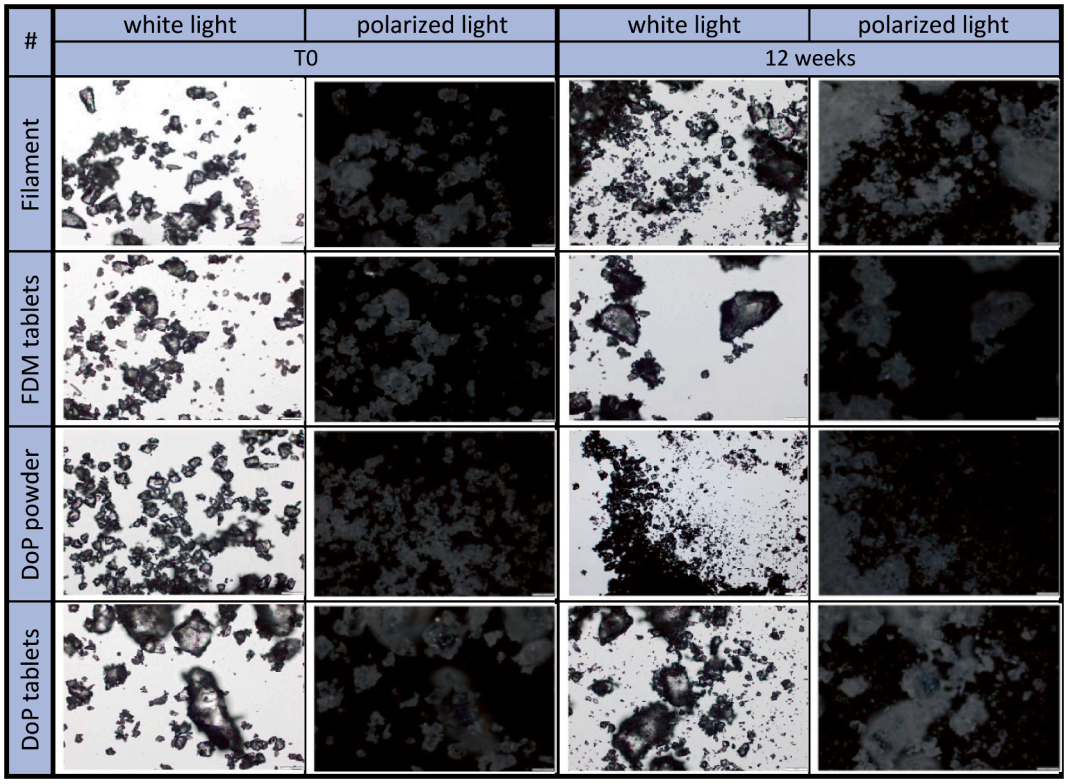

Fig. 3. Microscopic images of ground filament, tablets and DoP powder at 10× magnification at T0 and after twelve weeks of storage at 40 °C in desiccator (images of DoP tablets from Gottschalk et al., 2022b).

Non-sink dissolution (Fig. 4) confirmed the presence of small crystalline traces in DoP printed tablets as the supersaturation declined faster (101 µg/mL after 120 min dissolution for stability samples before storage) compared to the other materials (161–181 µg/mL after 120 min dissolution for stability samples before storage). Anwar et al. (2015) described that the presence of small crystal nuclei can induce precipitation in a supersaturated solution. Similar supersaturation profiles were obtained for stored samples, indicating no further recrystallization. There was only one exception in case of FDM tablets after two weeks of storage, where supersaturation reduced faster. It is likely that this was due to content fluctuations in the filament, which will be discussed in the following section. Since the material was ground and homogenized for non-sink dissolution, error bars were low.

The storage conditions might have contributed to the good physical stability of the material. Samples had been stored at 40 °C in a desiccator, since pretests had shown that storage at 75% r.h. led to strong recrystallization due to water sorption. Copovidone is known to be a hygroscopic polymer. Humidity in an ASD can lower the glass transition temperature (T_g) and increase the mobility of the API facilitating recrystallization (Patel and Serajuddin, 2022). However, storage at elevated temperature and dry conditions resulted in subsequent drying of the materials, indicated by an increase of T_g (Table 3) in all cases. The T_g was lowest for DoP tablets, which can be attributed to the use of a water-based ink and residual moisture.

3.4. Content and drug release

In order to ensure the correct dose of 3D printed SODFs, it is necessary that the API is well distributed in the polymer matrix. Local supersaturations of API in the polymer can further lead to enhanced recrystallization. The content and content uniformity were evaluated during the whole process chain. Table 4 displays the blend content prior extrusion, the filament content and the content of the remaining material in the feeder after extrusion. The mean content of the blend was slightly higher than the targeted content but also showed high deviations. This was probably related to the high differences in particles size of the different material. The particle size of KTZ ranged between 1 and 5 µm whereas in case of copovidone particles up to 200 µm were observed using a microscope. We observed a significant increase ($p < 0.05$) of drug content of the remaining material in the feeder and a significant decrease of filament content during extrusion ($p < 0.05$), indicating segregation of the powder blend during extrusion. It is likely that due to the cohesiveness of the smaller KTZ particles and adhesion to the feeder walls, small portions of KTZ remained in the extruder, thereby reducing the filament content and increasing the content of the remaining powder material in the feeder. This is supported by an increase of powder screw speed from approx. 25 rpm to 29 rpm towards the end of extrusion. Since extrusion was performed approximately 40 °C below the degradation temperature of KTZ (221 °C, Kanaujia et al. (2011)) and no impurities were observed in UPLC chromatograms, it is unlikely that content decrease was due to degradation.

Content of feedstock materials and tablets are displayed in Fig. 5. In two cases, the deviations of FDM tablets and filaments were higher compared to the other samples (ranging from 3.5 to 6.6%), indicating inhomogeneities in the filament. Content deviations were very low for DoP powder material and DoP tablets being mainly in a range of <1% (with a maximum of 2.7%). DoP powder material was milled post extrusion and blended, which probably contributes to the content uniformity.

The mean content of DoP powder and tablets was in all cases lower than the targeted content, whereas FDM filament and tablet content was higher in many cases. Comparing the feedstock materials, DoP powder showed a significantly lower content than the filament at T0 ($p < 0.05$). It is likely that the increased powder surface of the DoP powder accelerated water sorption during handling and intermittent storage of the samples as no indications on drug degradation were observed. Water sorption increases the tablet mass and leads to a lower apparent drug content. Filaments on the other hand, have a lower surface area-to

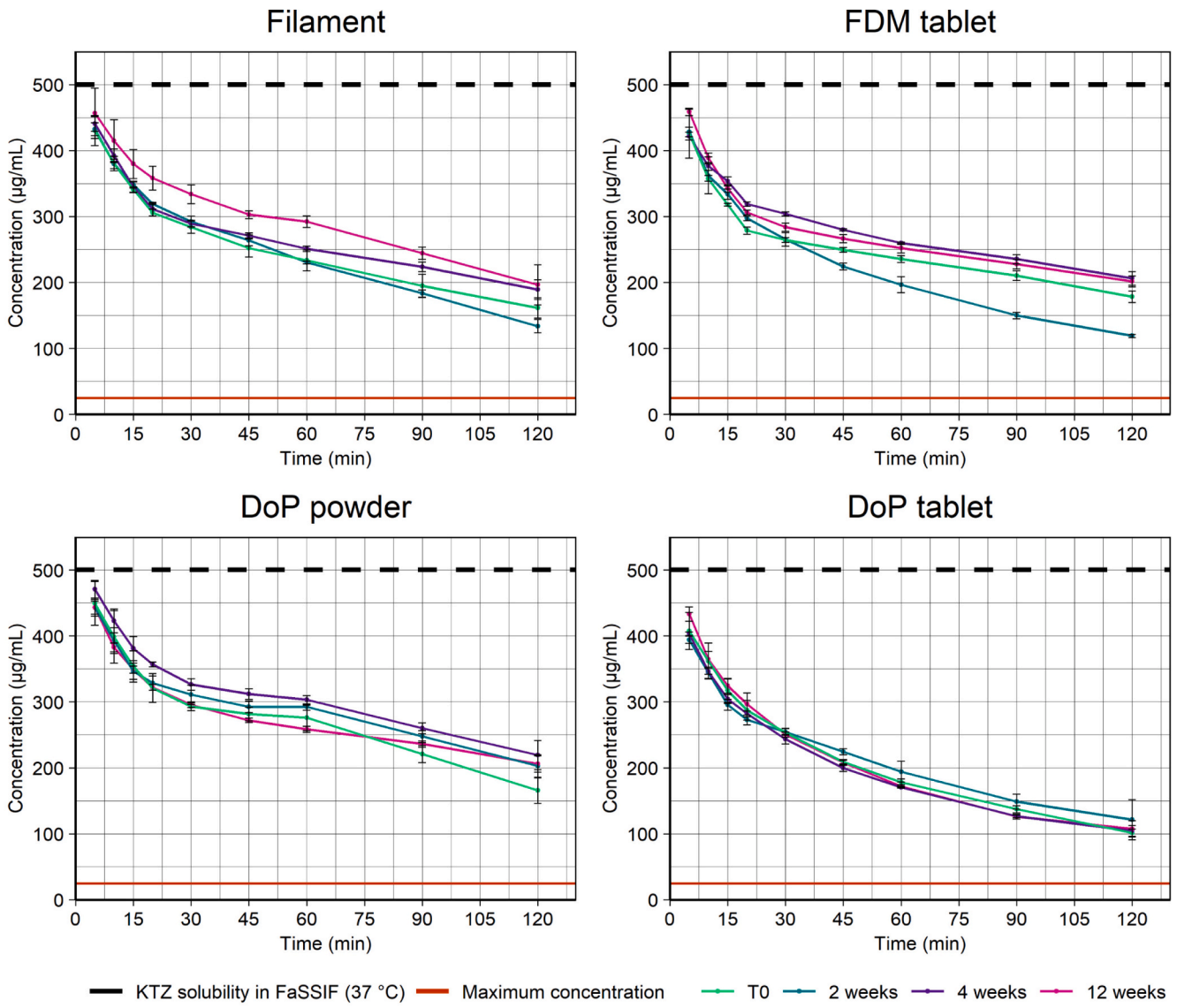

Fig. 4. Non-sink dissolution of filament, tablets and DoP powder (mean concentration ± SD, $n = 3$).

Table 3
T_gs of materials during storage.

Samples	T_g (°C) ± SD ($n = 3$)			
	Filament	FDM tablet	DoP powder	DoP tablet
T0	51.9 ± 4.4	55.5 ± 2.4	54.2 ± 0.9*	34.0 ± 12.1*
2 weeks	59.1 ± 0.5	61.6 ± 0.3	66.5 ± 4.5	58.3 ± 0.5
4 weeks	66.6 ± 1.1	65.1 ± 2.2	56.1 ± 9.9	64.2 ± 0.7
12 weeks	68.3 ± 1.5	72.3 ± 1.0	74.6 ± 0.4	69.4 ± 0.6*

* Data were shown in previous study (Gottschalk et al., 2022a).

Table 4
Content of powder blend, filament and of blend in feeder after extrusion (Mean ± SD).

	Blend	Filament	Feeder after extrusion
	($n = 12$)	($n = 9$)	($n = 3$)
Content (%)	103.6 ± 1.8	98.6 ± 1.3	106.0 ± 0.8

volume ratio slowing down water sorption. Furthermore, the drug content of DoP printed tablets at T0 was significantly lower ($p < 0.05$) than drug content of the DoP tablets, whereas no significant differences were observed after storage of the samples. Printing was performed using a water-based ink and it is likely that water remained in the tablets. The drying process was not optimized in this study. Samples post-dried during storage, which is also supported by the increasing T_g of the samples (Table 3).

Drug release from tablets was fast and all dosage forms released 80% of KTZ within 15–30 min (Fig. 6). Drug release was similar even though DoP tablets had a higher porosity. Copovidone is a well soluble polymer and KTZ was amorphous. Fast dissolution and the small size of the tablets are possibly the reason that no differentiation was possible. Both types of tablets eroded in a similar manner upon contact with the dissolution medium. It is likely that in case of DoP tablets the dissolution medium led to swelling of the polymer on the tablet surface, making the dissolution independent from the tablet porosity. This effect was described for compressed amorphous melt extrudate by Flügel et al. (2021).

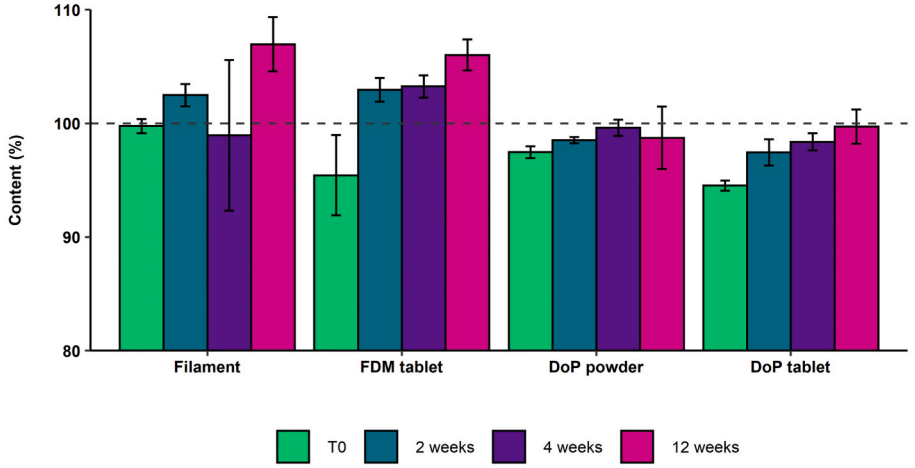

Fig. 5. KTZ content for filament, tablets and DoP powder (mean drug content ± SD, n = 3).

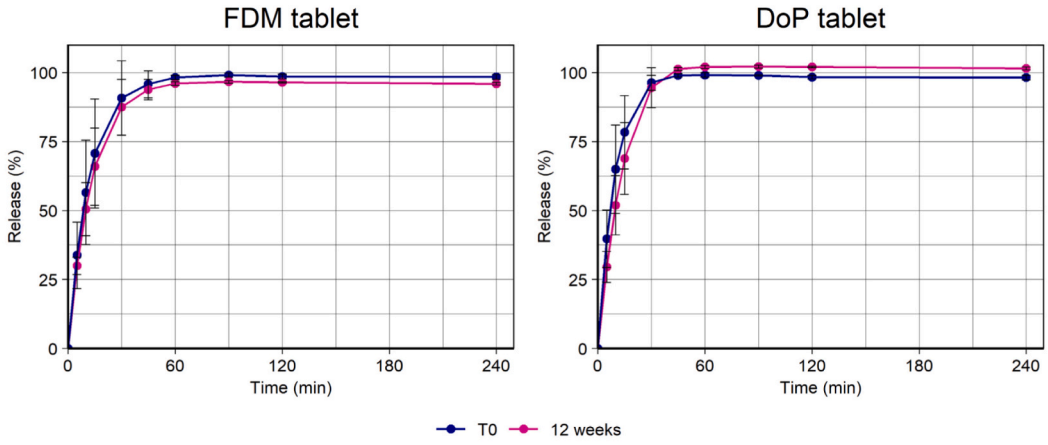

Fig. 6. Sink-dissolution of FDM and DoP tablets (mean release ± SD, n = 3).

3.5. Comparison of techniques

The choice on which 3DP techniques to employ depends greatly on the material properties. In case of a brittle formulation, the filament production and printability will be more difficult and may require additional equipment to enable printing. Furthermore, the production of filaments is challenging, especially the production of amorphous filament at high drug loads, as the parameter settings for ASDs (high screw speeds) and filament (low screw speeds) can be contradicting and need extensive investigation of a sweet spot. Several techniques have been employed to bypass the step of filament production by, e.g., direct powder extrusion (Goyanes et al., 2019; Zheng et al., 2021) or modification of the feeding mechanism (Gottschalk et al., 2021). Nevertheless, the use of filament as an intermediate is especially beneficial for production of dosage forms as the solid state reduces the risk of operator exposure (Quodbach et al., 2021). However, even though the material in this study was in a solid state, it imposes the risk of small splinters during handling of the filament or detaching tablets from the build plate when material is too brittle.

In case of an ASD being to brittle for FDM, DoP printing presents a suitable alternative printing technique. However, an additional milling step is necessary to achieve printable powder bed material. To reduce the number of processing steps and further bypass thermal stress during HME, also the use of spray-dried ASDs would be conceivable. Still, a thorough assessment of possible inks and printing parameters is necessary (Gottschalk et al., 2022a). The high surface area combined with high hygroscopicity of copovidone presented a challenge during the manufacturing process, which makes it necessary to perform manufacturing at controlled conditions. Furthermore, a powder-based process naturally requires additional safety precautions. On the other hand, milling of extrudate is easier than the production of homogenous filaments for FDM printing and formulation development is facilitated as the process is mainly independent from the mechanical properties of the formulation.

In DoP, the printability of customized inks was reported to present a major challenge and intensive formulation development is required to achieve optimal properties in terms of surface tension, viscosity and density (Prasad and Smyth, 2016). This study used a simple ink composition, which occasionally led to malfunction of individual nozzles, wherefore it was necessary to replace the print cartridge. This was sufficient for the number of tablets produced in this study. Three cartridges were used to print the whole number of tablets. At a larger scale, the ink needs to be optimized for the respective printhead in order to ensure the longevity of printheads. In addition, this study used organic solvents in the ink composition to ensure faster evaporation and prevent recrystallisation. The presence of residual amounts of solvent in the tablets is likely, wherefore, tablets would have to be additionally tested to meet the limits of the ICH Q3C (R8) on residual solvents in pharmaceuticals. In this study a mixture of ethanol and water was used. Ethanol, being a class 3 solvents, is a solvent with low toxic potential. However, the comparison in the prior study indicated that the higher volatile solvent methanol resulted in less recrystallization at higher drug loads.

The use of more volatile solvents may be necessary to increase the drug loading or for APIs with a higher recrystallization tendency. Furthermore, residual water was not fully removed during drying. Drying of tablets is a critical process and the impact of residual moistures in the DoP tablets should be further investigated.

Great differences between the two techniques are the appearance and dimensional properties of the tablets. FDM tablets showed poor resolution compared to DoP printed tablets. The resolution in DoP printing is mainly dependent on the particle size of the powder material (Infanger et al., 2019) whereas the resolution in FDM depends on the nozzle size (Kiński and Pietkiewicz, 2020) and the viscosity of molten material. A nozzle with a diameter of 0.4 mm was used in this study. Smaller nozzles are available but it has to be considered that this would also result in a higher printing duration. The poor resolution of FDM tablets has been widely described (Brambilla et al., 2021) and a study among children revealed that FDM tablets were favored least compared to tablets produced by selective laser sintering, semi-solid extrusion and digital light processing due to their rough and hard appearance (Januskaite et al., 2020). This eventually results in impaired patient compliance wherefore printing parameters and tablet geometries in FDM have to be chosen wisely and might require post-processing. Contributing to that, tablet mass variations of FDM tablets were higher compared to DoP in most batches, which was possibly a result of the filament quality. As filament extrusion is very challenging another approach could be to optimize FDM printers for the production of SODFs by equipping them with control mechanism that adapt to changes in filament diameter and deposited mass. DoP tablets were not as dense as FDM tablets due to the lower bulk density of the powder bed. Higher porosity can be beneficial regarding API release but also challenging when high doses of API have to be applied. Several approaches have been reported for powder-based printing processes to increase powder material density, such as the use of powder with bimodal particle size distribution (Sofia et al., 2018). From these observations we conclude that FDM tablets are rather suited when high doses have to be applied due to their higher mass-to-volume ratio, whereas DoP tablets are suited for the application of porous systems. For both printing techniques, the 3D design has to be adapted to the respective material density to achieve the required dose.

Both 3DP techniques were capable in producing amorphous and physically stable SODFs. It has to be pointed out, though, that even small traces of crystallinity, as in the case of DoP tablets, resulted in a slightly impaired supersaturation performance, which may reduce oral absorption. The DoP technique is prone to recrystallization when using an ASD as powder bed material wherefore very high drug loads might be difficult to achieve. Higher drug loads are likely feasible in FDM but the effects of the API on the processing conditions and mechanical properties of filaments have to be considered.

The storage stability of the feedstock materials is more important than the stability of 3D printed tablets, as tablets for on-demand production will not have long shelf-life. With FDM, the quality of filaments during storage must be ensured, to prevent changes in terms of dimensional and mechanical properties such as embrittlement, which was observed in this study.

In FDM, a homogenous drug distribution in the filament is crucial since inhomogeneities in filaments can result in over- or underdosing of tablets. This study indicated small variations of drug content uniformity in filaments produced on a small-scale extruder. However, at different extrusion setups or for different formulations, variations could be more pronounced and hence, more critical. In the event that blend segregation is likely to occure, it may be necessary to include a granulation step prior to extrusion to ensure content uniformity. For DoP printing, the usage of a hot melt extruded single-phase material is beneficial as content fluctuations can be balanced out by milling of the extrudate and subsequent homogenization. Another benefit is that segregation of DoP powder components during the manufacturing process is not possible since the API is embedded in the polymer. Even though it appears that optimization of the extrusion process is not as necessary as in FDM, it is also important in DoP printing of ASDs that the API is equally distributed in the polymer as local supersaturations will recrystallize to a greater degree upon contact with the ink.

The choice of 3DP technique will also depend on the respective API. Due to FDM printing being a thermo-intensive process, degradation of temperature-sensitive APIs may be possible. If water-based inks are used in DoP, this will present a challenge to APIs sensitive to hydrolysis. These two scenarios were not covered in this study.

4. Conclusion

In this study, we demonstrated that printing of an ASD was successful using the printing techniques FDM and DoP printing. Tablets with a high drug loading were achieved in which the API was amorphous and physically stable. We elaborated on the advantages and drawbacks of each printing technique and the respective aspects that have to be considered in the manufacturing process. If mechanical properties allow the production of flexible filaments, FDM is preferable for the production of high dose ASDs due to the lower chances of recrystallization. It has to be considered, though, that production of filament is challenging and operators should pay particular attention to filament uniformity. DoP printing presents a good alternative for brittle ASDs. DoP tablets were further advantageous compared to FDM tablets in terms of mass uniformity. However, high drug loaded ASDs and formulations that are sensitive to moisture and recrystallization will be difficult to be printed with DoP printing as well as high doses due to the higher porosity of SODFs. The choice of manufacturing process with an ASD depends on the API, targeted dose and physical stability in the respective polymer matrix. Each 3DP technique has its potential that can be leveraged for different applications.

Funding

Parts of this work were supported by the German Ministry of Education and Research [grant number 13XP5064].

CRediT authorship contribution statement

Nadine Gottschalk: Conceptualization, Investigation, Methodology, Formal analysis, Writing – original draft, Visualization. **Malte Bogdahn:** Conceptualization, Supervision, Writing – review & editing. **Julian Quodbach:** Conceptualization, Supervision, Writing – review & editing.

Declaration of Competing Interest

The authors declare the following financial interests/personal relationships which may be considered as potential competing interests:

Malte Bogdahn has patent Process for the manufacture of a solid pharmaceutical administration form pending to Merck Patent GmbH. Julian Quodbach has patent Process for the manufacture of a solid pharmaceutical administration form pending to Merck Patent GmbH. Nadine Gottschalk has patent Process for the manufacture of a solid pharmaceutical administration form pending to Merck Patent GmbH.

Data availability

No data was used for the research described in the article.

Acknowledgements

The authors would like to thank Marcel Wedel for his technical support during the DoP experiments and Alessandro-Giuseppe Elia for his support during hot-melt extrusion. The authors would also like to thank the German Federal Ministry of Education and Research, as parts

of this work were funded through the initiative ProMatLeben (grant number 13XP5064).

Appendix A. Supplementary data

Supplementary data to this article can be found online at https://doi.org/10.1016/j.ijpx.2023.100179.

References

Alhijjaj, M., Nasereddin, J., Belton, P., Qi, S., 2019. Impact of processing parameters on the quality of pharmaceutical solid dosage forms produced by Fused Deposition Modeling (FDM). Pharmaceuticals 11, 633. https://doi.org/10.3390/pharmaceutics11120633.

Antic, A., Zhang, J., Amini, N., Morton, D.A.V., Hapgood, K.P., Ft, F., 2021. Screening pharmaceutical excipient powders for use in commercial 3D binder jetting printers. Adv. Powder Technol. 32, 2469–2483. https://doi.org/10.1016/j.apt.2021.05.014.

Anwar, J., Khan, S., Lindfors, L., 2015. Secondary crystal nucleation: Nuclei breeding factory uncovered. Angew. Chem. Int. Ed. 54, 14681–14684. https://doi.org/10.1002/anie.201501216.

Araújo, M.R.P., Sa-barreto, L.L., Gratieri, T., Gelfuso, G.M., Cunha-filho, M., 2019. The digital pharmacies era: How 3D Printing technology using fused deposition modeling can become a reality? Pharmaceutics 11, 128. https://doi.org/10.3390/pharmaceutics11030128.

Brambilla, C.R.M., Okafor-muo, O.L., Hassanin, H., Elshaer, A., 2021. 3DP printing of oral solid formulations: a systematic review. Pharmaceutics 13. https://doi.org/10.3390/pharmaceutics13030358.

Buyukgoz, G.G., Kossor, C.G., Davé, R.N., 2021. Enhanced supersaturation via fusion-assisted amorphization during fdm 3d printing of crystalline poorly soluble drug loaded filaments. Pharmaceutics 13. https://doi.org/10.3390/pharmaceutics13111857.

Chamberlain, R., Windolf, H., Geissler, S., Quodbach, J., Breitkreutz, J., 2022. Precise dosing of pramipexole for low-dosed filament production by hot melt extrusion applying various feeding methods. Pharmaceutics 14, 216. https://doi.org/10.3390/pharmaceutics14010216.

Chang, S., Jin, J., Yan, J., Dong, X., Chaudhuri, B., 2021. Development of a pilot-scale HuskyJet binder jet 3D printer for additive manufacturing of pharmaceutical tablets. Int. J. Pharm. 605, 120791 https://doi.org/10.1016/j.ijpharm.2021.120791.

Clark, E.A., Alexander, M.R., Irvine, D.J., Roberts, C.J., Wallace, M.J., Yoo, J., Wildman, R.D., 2020. Making tablets for delivery of poorly soluble drugs using photoinitiated 3D inkjet printing. Int. J. Pharm. 578, 118805 https://doi.org/10.1016/j.ijpharm.2019.118805.

Flügel, K., Schmidt, K., Mareczek, L., Gäbe, M., Hennig, R., Thommes, M., 2021. Impact of incorporated drugs on material properties of amorphous solid dispersions. Eur. J. Pharm. Biopharm. 159, 88–98. https://doi.org/10.1016/j.ejpb.2020.12.017.

Fuenmayor, E., Forde, M., Healy, A., Devine, D., Lyons, J., McConville, C., Major, I., 2018. Material considerations for fused-filament fabrication of solid dosage forms. Pharmaceutics 10, 44. https://doi.org/10.3390/pharmaceutics10020044.

Gottschalk, N., Bogdahn, M., Harms, M., Quodbach, J., 2021. Brittle polymers in fused deposition modeling: an improved feeding approach to enable the printing of highly drug loaded filament. Int. J. Pharm. 597, 120216 https://doi.org/10.1016/j.ijpharm.2021.120216.

Gottschalk, N., Burkard, A., Quodbach, J., Bogdahn, M., 2022a. Drop-on-powder 3D printing of amorphous high dose oral dosage forms: process development, opportunities and printing limitations. Int. J. Pharm. X 100151. https://doi.org/10.1016/j.ijpx.2022.100151.

Gottschalk, N., Quodbach, J., Elia, A.-G., Hess, F., Bogdahn, M., 2022b. Determination of feed forces to improve process understanding of Fused Deposition Modeling 3D printing and to ensure mass conformity of printed solid oral dosage forms. Int. J. Pharm. 614, 121416 https://doi.org/10.1016/j.ijpharm.2021.121416.

Goyanes, A., Allahham, N., Trenfield, S.J., Stoyanov, E., Gaisford, S., Basit, A.W., 2019. Direct powder extrusion 3D printing: fabrication of drug products using a novel single-step process. Int. J. Pharm. 567, 118471 https://doi.org/10.1016/j.ijpharm.2019.118471.

Ilyés, K., Kovács, N.K., Balogh, A., Borbás, E., Farkas, B., Casian, T., Marosi, G., Tomuță, I., Nagy, Z.K., 2019. The applicability of pharmaceutical polymeric blends for the fused deposition modelling (FDM) 3D technique: Material considerations–printability–process modulation, with consecutive effects on in vitro release, stability and degradation. Eur. J. Pharm. Sci. 129, 110–123. https://doi.org/10.1016/j.ejps.2018.12.019.

Infanger, S., Haemmerli, A., Iliev, S., Baier, A., Stoyanov, E., Quodbach, J., 2019. Powder bed 3D-printing of highly loaded drug delivery devices with hydroxypropyl cellulose as solid binder. Int. J. Pharm. 555, 198–206. https://doi.org/10.1016/j.ijpharm.2018.11.048.

Jamróz, W., Szafraniec, J., Kurek, M., Jachowicz, R., 2018. 3D printing in pharmaceutical and medical applications – recent achievements and challenges. Pharm. Res. https://doi.org/10.1007/s11095-018-2454-x.

Januskaite, P., Xu, X., Ranmal, S.R., Gaisford, S., Basit, A.W., Tuleu, C., Goyanes, A., 2020. I spy with my little eye: a paediatric visual preferences survey of 3d printed tablets. Pharmaceutics 12, 1–16. https://doi.org/10.3390/pharmaceutics12111100.

Kanaujia, P., Lau, G., Ng, W.K., Widjaja, E., Hanefeld, A., Fischbach, M., Maio, M., Tan, R.B.H., 2011. Nanoparticle formation and growth during in vitro dissolution of ketoconazole solid dispersion. J. Pharm. Sci. 100, 2876–2885. https://doi.org/10.1002/jps.22491.

Keen, J.M., Martin, C., MacHado, A., Sandhu, H., McGinity, J.W., Dinunzio, J.C., 2014. Investigation of process temperature and screw speed on properties of a pharmaceutical solid dispersion using corotating and counter-rotating twin-screw extruders. J. Pharm. Pharmacol. 66, 204–217. https://doi.org/10.1111/jphp.12106.

Kiński, W., Pietkiewicz, P., 2020. Influence of the printing nozzle diameter on tensile strength of produced 3D models in FDM technology. Agric. Eng. 24, 31–38. https://doi.org/10.1515/agriceng-2020-0024.

Kissi, E.O., Nilsson, R., Nogueira, L.P., Larsson, A., Tho, I., 2021. Influence of drug load on the printability and solid-state properties of 3D-printed Naproxen-based amorphous solid dispersion. Molecules 26, 4492. https://doi.org/10.3390/molecules26154492.

Melocchi, A., Parietti, F., Maroni, A., Foppoli, A., Gazzaniga, A., Zema, L., 2016. Hot-melt extruded filaments based on pharmaceutical grade polymers for 3D printing by fused deposition modeling. Int. J. Pharm. 509, 255–263. https://doi.org/10.1016/j.ijpharm.2016.05.036.

Nasereddin, J.M., Wellner, N., Alhijjaj, M., Belton, P., Qi, S., 2018. Development of a simple mechanical screening method for predicting the feedability of a pharmaceutical FDM 3D printing filament. Pharm. Res. 35, 151. https://doi.org/10.1007/s11095-018-2432-3.

Patel, N.G., Serajuddin, A.T.M., 2022. Moisture sorption by polymeric excipients commonly used in amorphous solid dispersion and its effect on glass transition temperature: I. Polyvinylpyrrolidone and related copolymers. Int. J. Pharm. 616, 121532 https://doi.org/10.1016/j.ijpharm.2022.121532.

Ponsar, H., Wiedey, R., Quodbach, J., 2020. Hot-melt extrusion process fluctuations and their impact on critical quality attributes of filaments and 3D-printed dosage forms. Pharmaceutics 12, 511. https://doi.org/10.3390/pharmaceutics12060511.

Prasad, L.K., Smyth, H., 2016. 3D Printing technologies for drug delivery: a review. Drug Dev. Ind. Pharm. https://doi.org/10.3109/03639045.2015.1120743.

Prasad, E., Islam, M.T., Goodwin, D.J., Megarry, A.J., Halbert, G.W., Florence, A.J., Robertson, J., 2019. Development of a hot-melt extrusion (HME) process to produce drug loaded AffinisolTM 15LV filaments for fused filament fabrication (FFF) 3D printing. Addit. Manuf. 29, 100776 https://doi.org/10.1016/j.addma.2019.06.027.

Quodbach, J., Bogdahn, M., Breitkreutz, J., Chamberlain, R., Eggenreich, K., Elia, A.G., Gottschalk, N., Gunkel-Grabole, G., Hoffmann, L., Kapote, D., Kipping, T., Klinken, S., Loose, F., Marquetant, T., Windolf, H., Geißler, S., Spitz, T., 2021. Quality of FDM 3D printed medicines for pediatrics: considerations for formulation development, filament extrusion, printing process and printer design. Ther. Innov. Regul. Sci. https://doi.org/10.1007/s43441-021-00354-0.

Raijada, D., Genina, N., Fors, D., Wisaeus, E., Peltonen, J., Rantanen, J., Sandler, N., 2013. A step toward development of printable dosage forms for poorly soluble drugs. J. Pharm. Sci. 102, 3694–3704. https://doi.org/10.1002/jps.23678.

Shah, N., Sandhu, Ha, Choi, D.S., Chokshi, H., Malick, A.W. (Eds.), 2014. Dissolution of Amorphous Solid Dispersions: Theory and Practice. Springer. https://doi.org/10.1007/978-1-4939-1598-9_15.

Sofia, D., Chirone, R., Lettieri, P., Barletta, D., Poletto, M., 2018. Selective laser sintering of ceramic powders with bimodal particle size distribution. Chem. Eng. Res. Des. 136, 536–547. https://doi.org/10.1016/j.cherd.2018.06.008.

Ting, J.M., Porter, W.W., Mecca, J.M., Bates, F.S., Reineke, T.M., 2018. Advances in polymer design for enhancing oral drug solubility and delivery. Bioconjug. Chem. 29, 939–952. https://doi.org/10.1021/acs.bioconjchem.7b00646.

Ullrich, A., Schiffter, H.A., 2018. The influence of polymer excipients on the dissolution and recrystallization behavior of ketoconazole: Application, variation and practical aspects of a pH shift method. Eur. J. Pharm. Biopharm. 133, 20–30. https://doi.org/10.1016/j.ejpb.2018.09.018.

Vaz, V.M., Kumar, L., 2021. 3D printing as a promising tool in personalized medicine. AAPS PharmSciTech 22, 49. https://doi.org/10.1208/s12249-020-01905-8.

Wang, Z., Han, X., Chen, R., Li, J., Gao, J., Zhang, H., Liu, N., Gao, X., Zheng, A., 2021. Innovative color jet 3D printing of levetiracetam personalized paediatric preparations. Asian J. Pharm. Sci. 16, 374–386. https://doi.org/10.1016/j.ajps.2021.02.003.

Wickström, H., Palo, M., Rijckaert, K., Kolakovic, R., Nyman, J.O., Määttänen, A., Ihalainen, P., Peltonen, J., Genina, N., de Beer, T., Löbmann, K., Rades, T., Sandler, N., 2015. Improvement of dissolution rate of indomethacin by inkjet printing. Eur. J. Pharm. Sci. 75, 91–100. https://doi.org/10.1016/j.ejps.2015.03.009.

Windolf, H., Chamberlain, R., Quodbach, J., 2021. Predicting drug release from 3D Printed oral medicines based on the surface area to volume ratio of tablet geometry. Pharmaceutics 13, 1453. https://doi.org/10.3390/pharmaceutics13091453.

Yu, D., Branford-White, C., Yang, Y.-C., Zhu, L., Welbeck, E.W., Yang, X., 2009. A novel fast disintegrating tablet fabricated by three-dimensional printing. Drug Dev. Ind. Pharm. 35, 1530–1536. https://doi.org/10.3109/03639040903059359.

Zhang, J., Feng, X., Patil, H., Tiwari, R.V., Repka, M.A., 2017. Coupling 3D printing with hot-melt extrusion to produce controlled-release tablets. Int. J. Pharm. 519, 186–197. https://doi.org/10.1016/j.ijpharm.2016.12.049.

Zheng, Y., Deng, F., Wang, B., Wu, Y., Luo, Q., Zuo, X., Liu, X., Cao, L., Li, M., Lu, H., Cheng, S., Li, X., 2021. Melt extrusion deposition (MEDTM) 3D printing technology – a paradigm shift in design and development of modified release drug products. Int. J. Pharm. 602, 120639 https://doi.org/10.1016/j.ijpharm.2021.120639.